ECS Transactions, 1 (8) 85-100 (2006)
10.1149/1.2214546, copyright The Electrochemical Society

COMSUMPTION OF PT CATALYST UNDER ELECTROLYSIS AND FUEL CELL OPERATION

Shuya Kawahara, Shigenori Mitsushima, Ken-ichiro Ota and Nobuyuki Kamiya

Department of Energy and Safety Engineering
Yokohama National University
79-5 Tokiwadai Hodogaya-ku Yokohama 240-8501
Japan

ABSTRACT

The relationship between the charge transfer of Pt dissolution reaction and the consumption has been investigated to clarify the dissolution mechanisms. It was determined using both the symmetric and asymmetric waves of potential. The charge of Pt oxidation was always larger than that of reduction. The difference of the oxidation and the reduction charges should be caused by the dissolution of Pt. From the relationship between the difference of the charges and the amount of the consumption, the electron number of Pt dissolution reaction was ca. 4. Therefore, the dissolution mechanism under the symmetric wave and asymmetric waves of the slow anodic / the fast cathodic sweep would be $Pt \rightarrow Pt^{4+} + 4e^-$. Pt consumption under asymmetric waves of the fast anodic / the slow cathodic sweep was enhanced, and this reaction would be $PtO_2 + 4H^+ + 2e^- \rightarrow Pt^{2+} + 2H_2O$. The dissolved Pt^{2+} was detected with the RRDE measurement.

INTRODUCTION

Pt catalyst has been widely used for electrochemical systems, i.e., fuel cells, water electrolyses and so on, because it has superior catalytic ability and high corrosion resistance.

Polymer electrolyte fuel cells (PEFCs) have been developed for applications such as vehicles and residential co-generation systems,[1-4] since PEFCs have high power density and low emission to environment. Conventional PEFCs have some problems of energy conversion efficiency and durability. Large overpotential and degradation of Pt catalyst for oxygen reduction reaction on cathode is a significant issue. Pt catalyst dissolves into electrolyte for long term operation, and particle size of Pt catalyst grows.[5-8]

A reliability and durability should be one of the most important key factors for commercialization.

Pt consumption in water electrolysis is proportional to the amount of charge in electrolysis for examples, the amount of consumption per charge is $5 \mu g A^{-1} h^{-1}$ in the sulfuric acid at $40^{o}C$.[9)] The consumption increases with the potential of an oxygen evolution electrode. However, the consumption rate under steady state in fuel cells should be very slow compared with water electrolysis as the electrode potential of fuel cells is lower than that of water electrolysis.

One of the key requirements is that the fuel cells must have a durability of frequent start-stop cycling. Before the startup of it, air is present on both of the anode and cathode due to leakage from outside air and/or crossover through the membrane. When hydrogen is introduced into the anode during startup, hydrogen occupies only part of the anode compartment. This makes the cathode potential rise, and causes carbon corrosion and oxygen evolution at the cathode electrode.[10)] In consequence, the Pt catalyst also might degrade severely. The effect of such a transitional state, i.e. potential range, sweep rate etc, on the consumption must be important owing to cycling of oxidation and reduction of Pt. This effect on the device such as fuel cells for vehicles and small size co-generation systems might be more serious than that on industrial uses because startup and shutdown would be often repeated in a short term on fuel cell systems.

Various mechanisms have been proposed to explain the dissolution of Pt with potential cycling. Kinoshita at el. suggested that Pt dissolved and the “real” surface area changed with potential cycling[11)]. Chemodanov and co-workers[12,13)] concluded that Pt dissolution occurred during the reduction of Pt surface oxides which was the same conclusion reached Johnson et al.[14)] using a rotating ring disk electrode to study the amount of soluble Pt^{2+} species formed. Rand and Woods[15)], on the other hand, concluded that Pt undergoes dissolution during the anodic portion of the potential cycling, based on the difference between the anodic and cathodic charge for Pt oxide formation and reduction. However, Pt consumption during transitional state wouldn’t be clarified enough, yet.

In this study, the relationship between the charge transfer of Pt dissolution reaction and the amount of Pt consumption has been investigated to clarify the mechanisms of Pt dissolution under transitional state.

EXPERIMENTAL

Pt consumption measurement experiment

A measurement of Pt consumption was carried out with a three-electrode electrochemical cell in 1M H_2SO_4 (JUNSEI KAGAKU, special grade) under nitrogen atmosphere at 40°C. Both the working and counter electrodes were made of 1cm^2 of the platinum wire (TANAKA KIKINNZOKU, 99.99%), and the reference electrode was the reversible hydrogen electrode (RHE). An amount of Pt consumption was measured from the weight change before and after the experiment. In this treatment, the Pt oxide was removed with hot hydrochloric acid (JYUNSEI KAGAKU, special grade). The behaviors of the potential and the current during the experiment were monitored with the oscilloscope (YOKOGAWADENKI model DL1620).

Potential of the working electrode was controlled by the symmetric triangular and rectangular waves as shown in Figure 1. A range of potential was controlled in two ways, i.e., the lower limit potential (E_L) was the range from 0.1 to 0.8V(vs. RHE) keeping the higher limit potential (E_H) 1.8V(vs. RHE), or E_H was range from 1.5 to 2.4V(vs. RHE) keeping E_L 0.5V(vs. RHE). The frequnecy of rectangular wave was from 5 to 100 Hz. The sweep rate of triangular wave was 20 to 100Vs^{-1} corresponding to from 5 to 50Hz in frequency. A number of the cycle was 900,000. The surface of the working electrode after the experiment was observed with the secondary electron microscopy (SEM, HITACHI model FB-2000A). Two types of asymmetric triangular waves were also applied as shown in Figure 2. One was 0.5Vs^{-1} of anodic sweep rate and 20Vs^{-1} of cathodic sweep rate, which was called asymmetry (A), and another was 20Vs^{-1} of anodic sweep rate and 0.5Vs^{-1} of the cathodic sweep rate, which was called asymmetry (B). Both of these conditions were corresponding to 0.37Hz in frequency.

Rotating ring-disk electrode measurement

Dissolved Pt ion was simultaneously detected with the Pt disk electrode (6mm diameter) / the Pt ring electrode (9mm outer diameter and 7mm inner diameter) in 1M H_2SO_4 at 40°C. The reference electrode was the reversible hydrogen electrode (RHE). The counter electrode was Pt which placed on the bottom of this cell.

Potential of the disk electrode was scanned from 0.05-1.5V(vs. RHE) under nitrogen atmosphere. An asymmetric triangular wave was applied to the disc electrode. One was 0.1Vs^{-1} of anodic sweep rate and 10Vs^{-1} of cathodic sweep rate, and another was 10Vs^{-1} of anodic sweep rate and 0.1Vs^{-1} of the cathodic sweep rate. Potential of ring electrode was at 0.4V or 1.5V(vs. RHE). The rotating ring disk electrode (RRDE) was rotated 400rpm using a rotating speed controller (NIKKOU KEISOKU). The potential was controlled with the bipotentiostat (HOKUTODENKO HA1020mM2B).

RESULTS AND DISCUSSION

Dependence of Pt consumption on the potential change range

Figure 3 shows the dependence of Pt consumption on E_H. The scan rate of the triangular wave was 100 Vs^{-1} corresponding to from 25 to 50Hz, and the frequency of the rectangular wave was 50 Hz. The consumption increased with E_H from 1.5 to 1.8V(vs. RHE) for both the triangular and rectangular waves. While E_H was more positive than 1.8V(vs. RHE), the amount of the consumption was constant. Figure 4 shows the relationship between reduction charge of Pt oxide and E_H. When E_H was more positive than 1.8V(vs. RHE), the reduction charge was constant. Therefore, the thickness of the Pt oxide layers reached constant, and the Pt consumption was also constant. For the rectangular wave, the amount of the consumption increased above 2.2V(vs. RHE) again. At this moment, the surface oxide layers dropped off. Therefore, the reduction charge of the Pt oxide decreased to from 2.2 to 2.4V(vs. RHE) as shown in Fig.4, and the large amount of Pt was consumed.

Figure 5 shows the dependence of Pt consumption on E_L. The maximum amount of the consumption was observed around 0.5V(vs. RHE) for both the triangular and the rectangular waves. This behavior would be affected by the oxide layers of the Pt surface.

It is generally known that two types of Pt oxides is called α-Pt oxide and β-Pt oxide by Shibata.[16,17] The α-Pt oxide forms under a moderate oxidation condition and reduces under wide potential range of 0.7-0.8V(vs. RHE). On the other hand, the oxide which reduces under potential range of the more negative and narrow is called β oxide. Figure 6 shows the linear sweep voltammogram of Pt electrode after it was oxidized at 0.5 Acm^{-2} for 30 minutes. The cathodic scan of the steady state cyclic voltammogram of Pt was also shown in the Fig. 6. Two peaks appeared at 0.6V and 0.2V(vs. RHE). This first peak was more negative potential and larger than that of the steady state cyclic voltammogram. Therefore, this would be corresponding to the mixture of α and β-Pt oxides. The second peak which had a large amount of charge would be corresponding to the polymer-like β-Pt oxide.[18-20]

The relationship between E_L and the reduction peak of Pt oxide will be discussed. Figure 7 shows the linear sweep voltammograms of Pt after 75,000 cycles of rectangular wave was applied. The cathodic scan of the steady state cyclic voltammogram of Pt was also shown in the Fig.7. E_H was 1.8V(vs. RHE), and E_L was 0.2, 0.5 and 0.65V(vs. RHE), respectively. The peak for 0.65V(vs. RHE) of E_L had 0.8 and 0.3V (vs. RHE) of the oxide reduction peaks. The potential of first peak was almost the same to that of the steady state cyclic voltammogram. Therefore, this peak would correspond to α-Pt oxide. The second peak had large amount of charge. This peak would correspond to β-Pt oxide. Other tow conditions had only first reduction peak of the oxide. The first peak for 0.2V(vs. RHE) of E_L was at more negative potential and had the larger amount of charge than that of others. Therefore, this peak would correspond to the mixture of α and β-Pt oxide. The first peak for 0.5V (vs. RHE) of E_L was at nearly same potential and the reduction charge of the oxide was equal to that of the steady state cyclic voltammogram.

Figure.8 shows the relationship between the amount of reduction charge of α and β-Pt oxide and E_L. When E_L was at the 0.65V(vs. RHE), the reduction charge of the oxide was the largest. Therefore, the oxide which was corrosion protective layers would be maintained on the surface. When E_L was at 0.5V(vs. RHE), the amount of the oxide layer was the least. Therefore, the corrosion protective layer of the surface would be the least at this potential. On the other hand, when E_L was 0.2V(vs. RHE), the reduction charge of the oxide was lager than that of 0.5V(vs. RHE). Therefore, the oxide was more maintained at 0.2V(vs. RHE) than at 0.5V(vs. RHE).

Figure 9 shows the SEM images after 30,000 cycles of the rectangular wave applied. E_H was 1.8V(vs. RHE) and E_L were 0.2, 0.5, and 0.65V(vs. RHE), respectively. The dendrite deposit was observed in Fig.9 (a). It would be dissolved Pt species in the electrolyte. There also appeared cubic type materials on Pt surface. Briss et al. suggested that the deposited material might inhibit the reduction of the Pt oxide in the region of the metal / oxide interface.[21,22)] Therefore, the cubic type materials might be Pt oxide which was prevented from reducing. The scraped-like surface was observed in Fig.9 (b). The polymer-like β-Pt oxide layers was observed in Fig.9 (c). The SEM observation of the Pt surface was a good correlation to the amount of the oxide layers.

As a conclusion, the rate of the formation of the protective oxide layers was the least around 0.5V(vs. RHE) of E_L. Therefore, the highest Pt consumption region had the least oxide layers and accelerated to the consumption.

<u>Dependence of Pt consumption on the potential rate</u>

The effect of the potential rate on the Pt consumption was investigated for both the symmetric triangular and the rectangular waves. E_L and E_H was 0.5 and 1.8V(vs. RHE), respectively. Figure 10 shows the dependence of Pt consumption on the frequency.

For the rectangular wave, the consumption was independence of the frequency, and the amount of the consumption was about 10ngcm^{-2}cycle^{-1}. Therefore, dissolution of Pt would occur during the potential step. On the other hand, the consumption increased with increasing the frequency up to 40Hz for the triangular wave. The amount of the consumption for the triangular wave from 20 to 40Hz was larger than that of the rectangular wave. If the frequency of the triangular wave was much higher, the consumption would be close to that of the rectangular wave. It might indicate the appropriate region of the frequency to give the maximum consumption.

Pt consumption under the asymmetric triangular wave

In order to clarify the effect of the direction of sweep on Pt consumption, the behavior of the consumption under the asymmetric triangular wave was investigated. The amount of the consumption was about 2ngcm^{-2}cycle^{-1} for the asymmetry (A). This value was almost the same to the symmetric triangular wave. On the other hand, that was about 20ngcm^{-2}cycle^{-1} for the asymmetry (B), and was about ten times larger than the asymmetry (A). This behavior might be caused by dissolution of the Pt oxide layers. By using RRDE measurement, we tried to confirm the dissolved Pt specie.

Figure 11 (a) shows the anodic sweep of the RRDE voltammogram under the asymmetry (A) at 1.5V of the potential of ring electrode. Figure 11 (b) shows the anodic sweep of the RRDE voltammogram under asymmetry (A) at 0.4V of the ring electrode. In the Fig.11 (a), no signal was detected by the ring electrode. In the Fig.11 (b), three reduction peaks were observed by the ring electrode. The peak C which appeared at the most positive potential of disk electrode would be the reduction current of oxygen which evolved at the disk electrode. The peak A which appeared at the most negative potential of disk electrode would be also reduction current of oxygen, because the cathodic sweep was very fast and this peak was not observed when E_H was 1.2V(vs. RHE). The peak B which appeared at 1.2V(vs. RHE) of the potential of disk electrode could not be identified. However, Laitinen and Enke suggested that this peak appeared according to the presence of absorbed oxygen-containing species by the platinum to produce the oxidized electrode state.[14)] Figure 12 (a) shows the cathodic sweep of the RRDE voltammogram under the asymmetry (B) at 1.5V of the potential of ring electrode, and Figure 12 (b) shows the cathodic sweep of the RRDE voltammogram under asymmetry (B) at 0.4V of the potential of the ring electrode. In the Fig.12 (a), an oxidation peak D was observed around 0.8V(vs. RHE) of the reduction potential of Pt oxide. In the Fig.12 (b), the peak E at the most negative potential would be an oxidation current of hydrogen which evolved at the disk electrode. The peak G which appeared at the most positive potential would be the reduction current of oxygen. The reduction current of the peak F was observed around 0.8V(vs. RHE). The peak D and F appeared around the reduction potential of the oxide. If Pt^{2+} dissolves during the reduction process, Pt^{2+} will oxidize by 1.5V of the potential of the ring electrode and reduce by 0.4V of the potential of the ring electrode. Therefore, the peak D and F would be Pt^{2+}.

Dissolution of Pt and Pt oxides

To determine the dissolution mechanisms of Pt under the transitional state, the relationship between the difference of the oxidation and reduction charges and the consumption will be discussed. Here, it was assumed that the difference of the oxidation and the reduction charges was the transfer of Pt dissolution reaction. Figure 13 shows the relationship between the difference of the charges and the amount of the consumption under various symmetric and asymmetric waves. Here, the slope was proportional to the electron number of the dissolution reaction.

$$n = (M_{Pt}/F) * (\Delta W/\Delta Q) \qquad [1]$$

Here, n, M_{Pt}, F, ΔW, and ΔQ were electron number of Pt dissolution reaction, molar weight of Pt, Faraday constant, weight loss of Pt electrode, difference of the oxidation and the reduction charges, respectively.

In the Fig.13, the solid line is for the symmetric wave and the slow anodic / the fast cathodic sweep (asymmetry (A)). The slope of this line indicates that the electron number of Pt dissolution reaction was ca. 4. Therefore, this dissolution reaction would be

$$Pt \rightarrow Pt^{4+} + 4e^- \qquad [2]$$

On the other hand, the dashed line is for the fast anodic / the slow cathodic sweep (asymmetry (B)) in the Fig.13. The slope of this line indicates that electron number of Pt dissolution reaction was ca. 2. Therefore, this dissolution reaction would be

$$PtO_2 + 4H^+ + 2e^- \rightarrow Pt^{2+} + 2H_2O \qquad [3]$$

Compared with $0.5Vs^{-1}$ of the symmetric triangular wave, the amount of consumption under the asymmetry (B) was larger. Therefore, the property of Pt oxide might be influenced by the rate of potential change.

CONCLUSION

The relationship between the amount of Pt consumption and the charge transfer of Pt dissolution reaction has been investigated to clarify the dissolution mechanisms. The most consumed potential range was between 0.5V(vs. RHE) of E_L and the more higher E_H. The highest consumption region had the least corrosion protective layers. As for the effect of the potential rate, the consumption increased with increasing the sweep rate. From the difference of between the oxidation and the reduction charges as a function of the consumption, the dissolution reaction under the symmetric waves and the slow anodic / the fast cathodic sweep (asymmetry (A)) would be $Pt \rightarrow Pt^{4+} + 4e^-$. The consumption was enhanced under the fast anodic / the slow cathodic sweep (asymmetry (B)). This dissolution would be $PtO_2 + 4H^+ + 2e^- \rightarrow Pt^{2+} + 2H_2O$. The dissolved Pt^{2+} was detected when Pt oxides was reduced. This enhanced dissolution was affected to not only the reduction condition but also the oxidation condition.

ACKNOWLEDEMENT

This study was supported by the project for "Research and Development of Polymer Electrolyte Fuel Cell" from the new Energy and Industrial Technology Development Organization (NEDO) of Japan.

REFERENCE

1) J. Adams and B. Bates, OHM, 54 (1999).
2) D. Elkaim, Abstract of 2000 Fuel Cell Seminar, p.491 (2000).
3) K. Shindo, T. Ouki, A. Fuju, O.Tajima, S. Yamamoto, T. susai, K.Tajima, Abstracts of 2000 of Fuel Cell Seminor, p.492 (2000).
4) M. Sperry, M. Tropey, Abstracts of 2000 Fuel cell Seminar, p.481(2000).
5) Mahlon S. Wilson, Frenando H. Garzon, Kurt E. Sickafus and Shimshon Gottesfeld, *J. Electrochem. Soc.*, **140** , 2872 (1993).
6) Akira Taniguchi, Tomoki Akita, Kazuaki Yasuda, Yoshinori Miyazaki, *J. Power Sources*, **130** , 42 (2004).
7) R. Mohatadi, W.-k. Lee, J.W. Van Zee, *J. Power Sources*, **138** , 216 (2004).
8) Robert M. Darling, Jeremy P. Meyers, *J. Electrochem. Soc.*, **150** , A1523 (2003).
9) S. Nishigori, K-I. Ota, and N. Kamiya, *J. Electroanal. Chem.*, **257** , 205 (1988).
10) Carl A. Reiser, Lawrence Bregoli, Timothy W. Patterson, Jung S. Yi, J. Deliang Yang, and Thomas D. Jarvi, *J. Electrochem. and Solid-State Letters*., **8**(6) , A273-A276 (2005).
11) K. Kinoshita, J. T. Lundquist, P. Stonehart, *J. Electroanal. Chem.*, **48** , 157 (1973)

12) A. N. Chemodanov, Y. M. Kolotyrkin, M. A. Dembrovskii, *Electrokhimiya*, **6** , 460 (1970)

13) A. N. Chemodanov, Y. M. Kolotyrkin, V. E. Kosmatyi, M. A. Dembrovskii, *Electrokhimiya,* **4** , 1466 (1968)

14) D. C. Johnson, D. T. Napp, S. Bruckenstein, *Electrochimica Acta*, **15** , 1493 (1970).

15) D. A. J. Rand, R. Woods, *J. Electroanal. Chem.*, **35** , 209 (1972)

16) S. Shibata, M.P. Sumino, *Elctrochimica. Acta*., **20 ,** 739 (1975).

17) S. Shibata, *J. Electroanal. Chem*., **89** , 37 (1978).

18) G. Tremiliosi-Filho, B.E. Conway, *Amercan. Chem. Soc*, vol. 8, No. 2, (1992).

19) Gottesfeld. S, Yanvi. M, Laser. D, *J. Electroanal. Chem*, **15** (1989).

20) S. J. Xia, V. I. Briss, *Electrichimica. Acta*., **44** , 467 (1998).

21) V. I. Briss, M. Chang, J.Segal, *J. Electroanal. Chem*., **355** , 181 (1993).

22) V. I. Briss, M. Goledzinowski, *J. Electroanal. Chem*., **351** , 227 (1993).

ECS Transactions, 1 (8) 85-100 (2006)

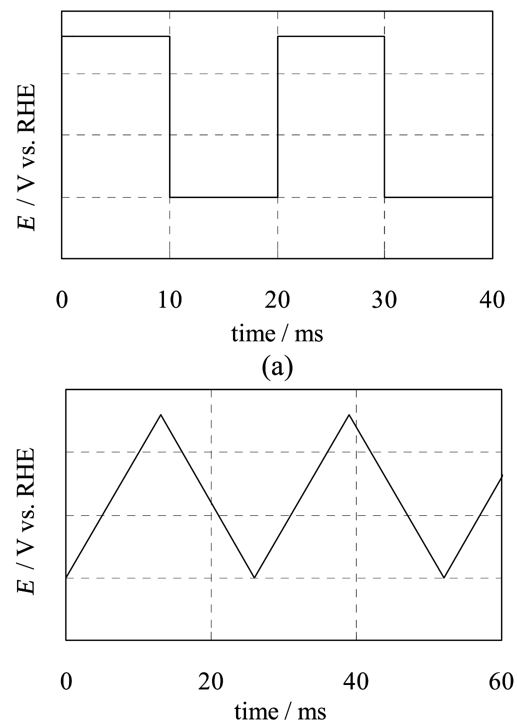

(b)

Fig.1 Profile of symmetric triangular and rectangular wave.
(a) symmetric rectangular wave, (b) symmetric triangular wave

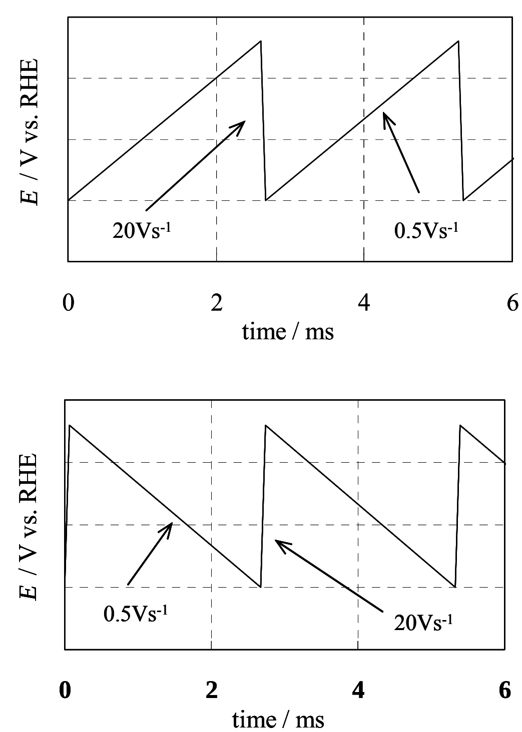

(b)

Fig.2 Profile of asymmetric triangular wave.
(a) asymmetry (A) , (b) asymmetry (B)

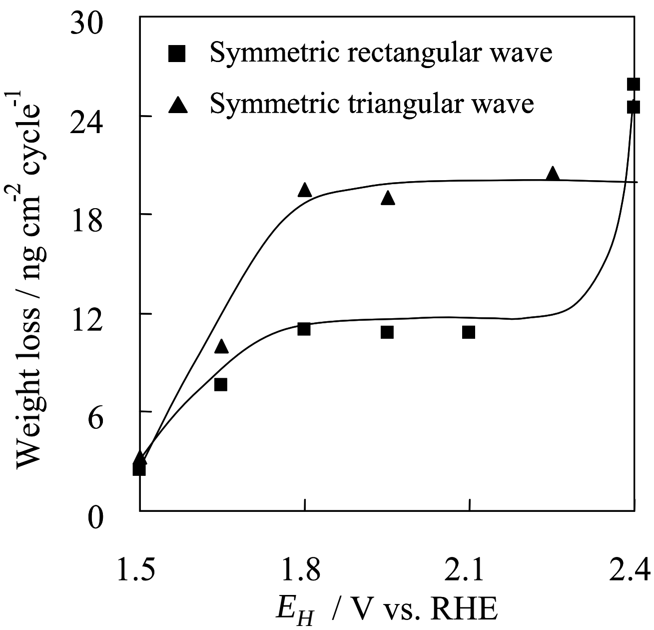

Fig.3 Dependence of Pt consumption on E_H keeping E_L 0.5V vs.RHE in H_2SO_4 under nitrogen atmosphere at 40°C.
frequency of triangular wave:25-50Hz, frequency of rectangular wave:50Hz

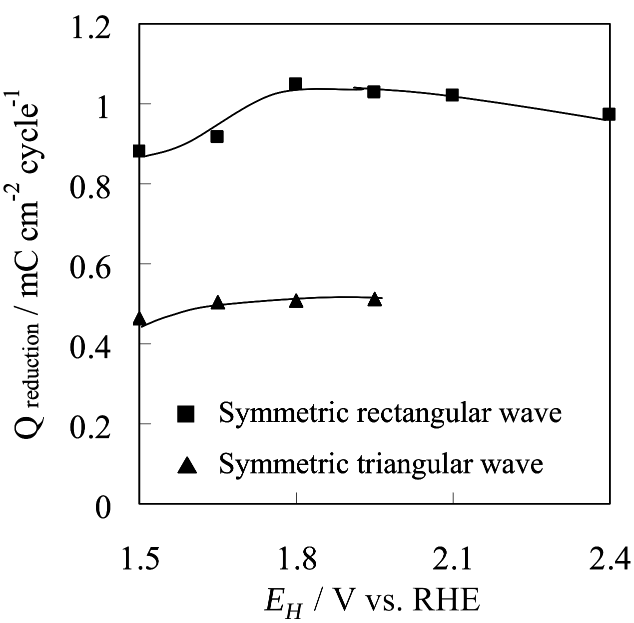

Fig.4 Relationship between the reduction charge for Pt oxide and E_H in H_2SO_4 under nitrogen atmosphere at 40°C.
E_L was 0.5V vs. RHE.

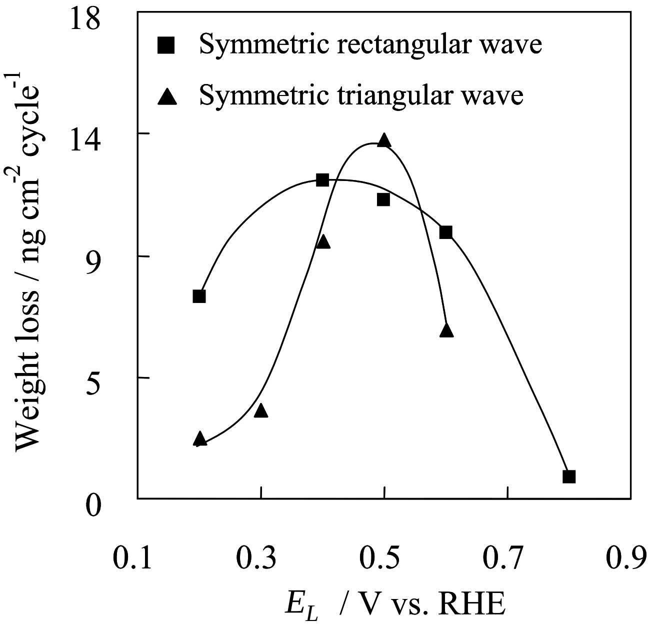

Fig.5 Dependence of Pt consumption on E_L keeping E_H 1.8V vs.RHE in H_2SO_4 under nitrogen atmosphere at 40°C.
frequency of triangular wave:25-50Hz, frequency of rectangular wave:50Hz

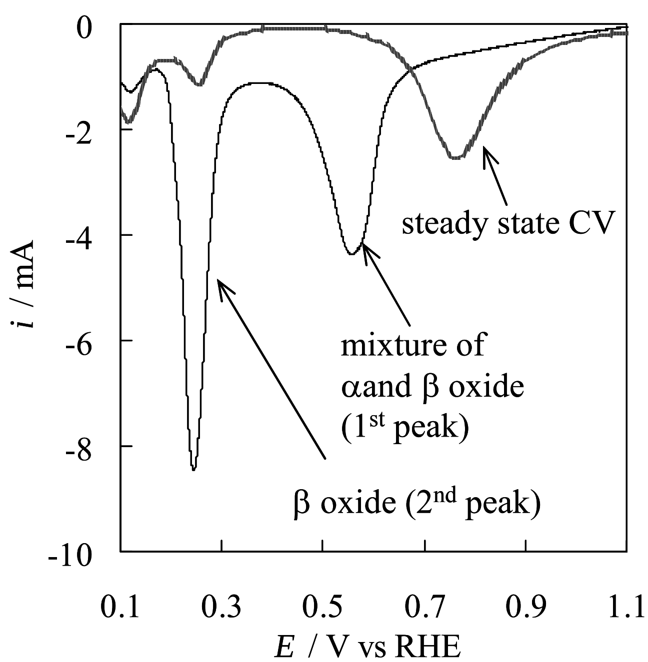

Fig.6 Linear sweep voltammogram for Pt at sweep rate $30mVs^{-1}$ in H_2SO_4 under nitrogen atmosphere at 40°C after Pt oxidized at $1.0Acm^{-2}$ for 30min.

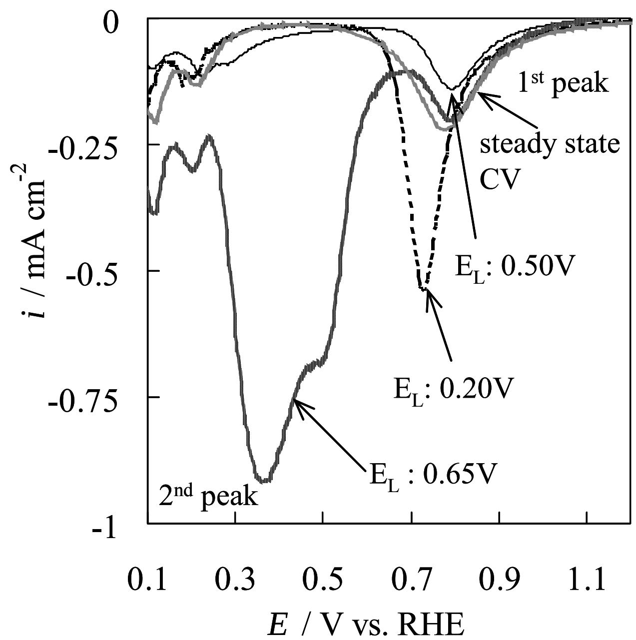

Fig.7 Linear sweep voltammograms for Pt at sweep rate 30mVs^{-1} in H_2SO_4 under nitrogen atmosphere at 40^oC after Pt oxidized by 75,000 cycles of the rectangular wave.

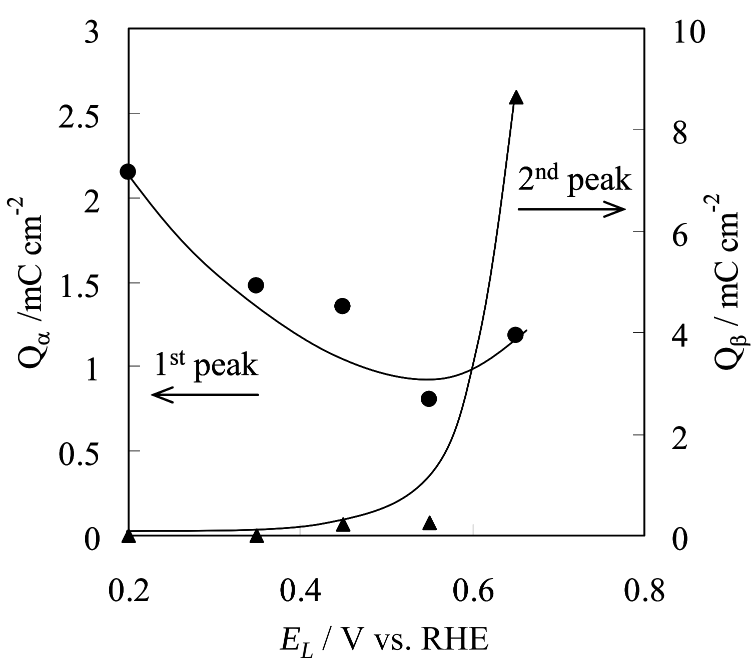

Fig.8 Relationship between the reduction charge for α-β Pt oxide and E_L after 75,000cycles of the rectangular wave applied.

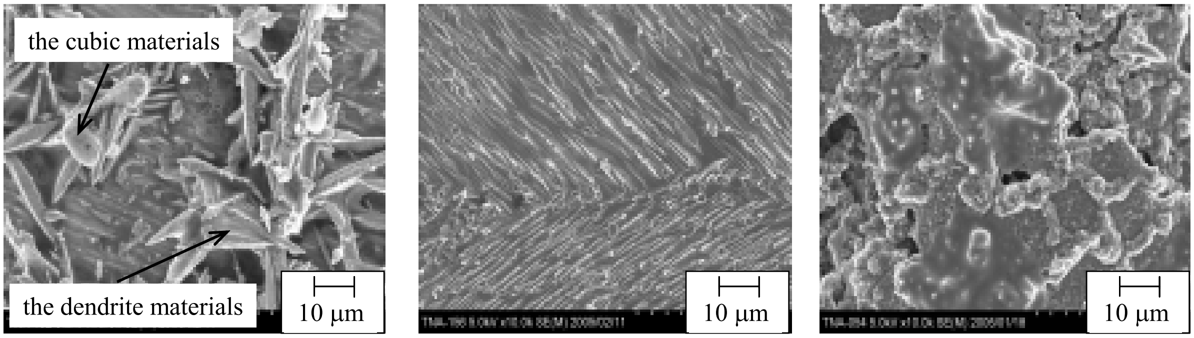

(a) E_L : 0.2V (b) E_L : 0.5V (c) E_L : 0.65V

Fig.9 SEM images of Pt electrode after consumption in H_2SO_4 at 40°C after 30,000 cycles of the rectangular wave applied.
potential range; (a) E_L : 0.2V, (b) E_L : 0.5V, (c) E_L : 0.65V.

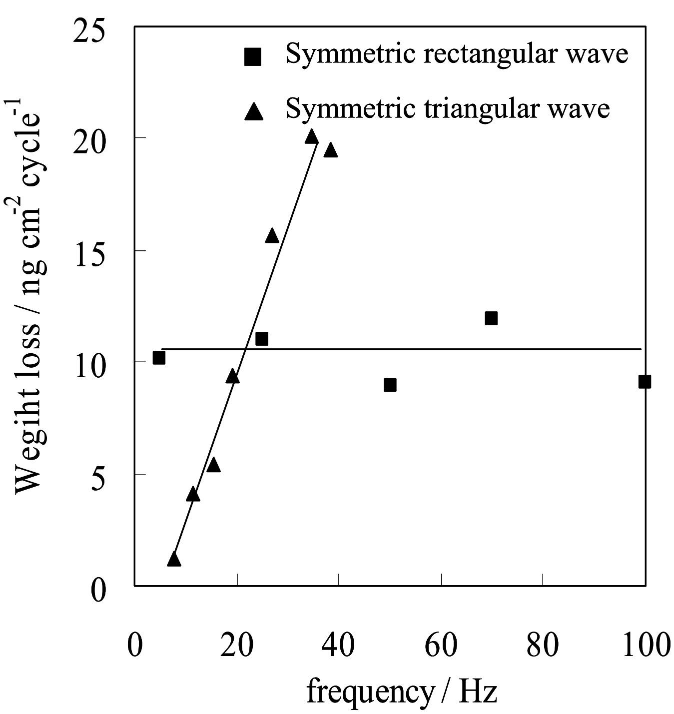

Fig.10 Dependence of Pt consumption on frequency in H_2SO_4 under nitrogen atmosphere at 40°C.
The potential range was 0.5 to 1.8V vs.RHE.

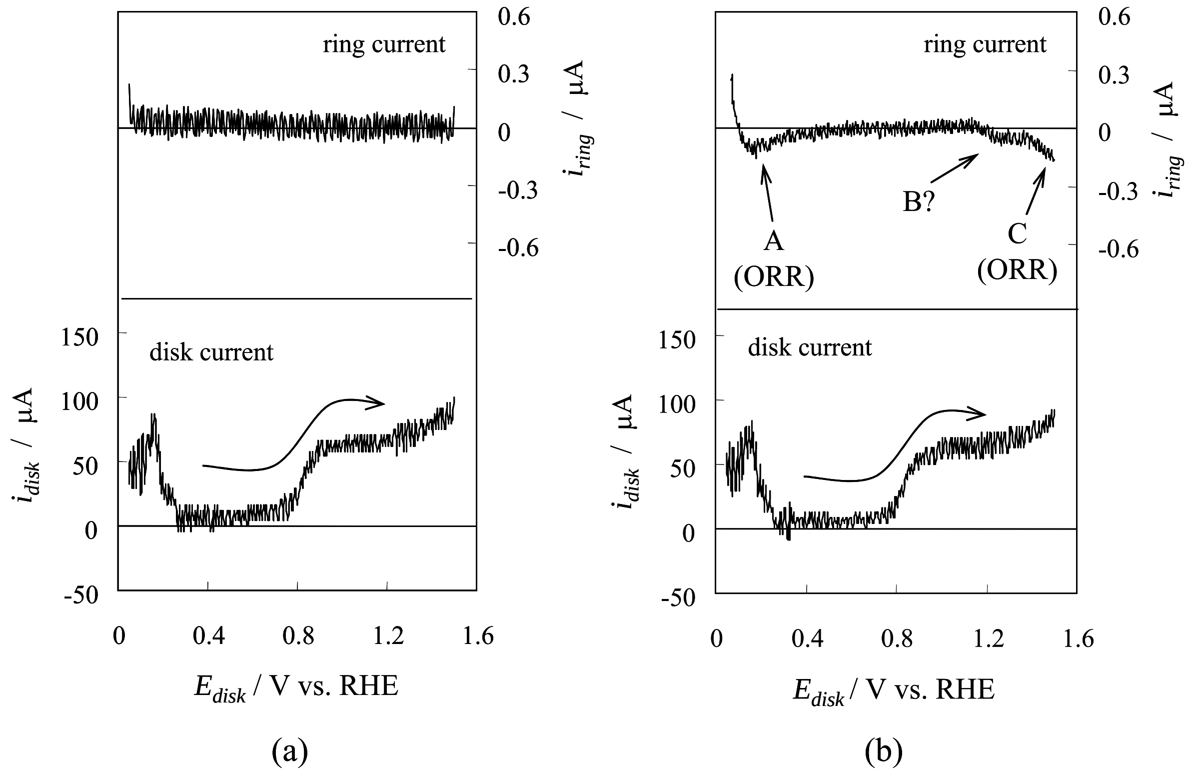

Fig.11 Anodic sweep of the cyclic voltammograms for Pt disk and ring electrode in H_2SO_4 under nitrogen atmosphere at 40^{o}C. The potential of Pt ring electrode was (a) 1.5V and (b) 0.4V.
potential range of disk electrode: 0.05-1.5V, anodic sweep rate; 0.1Vs^{-1}, cathodic sweep rate; 10Vs^{-1}

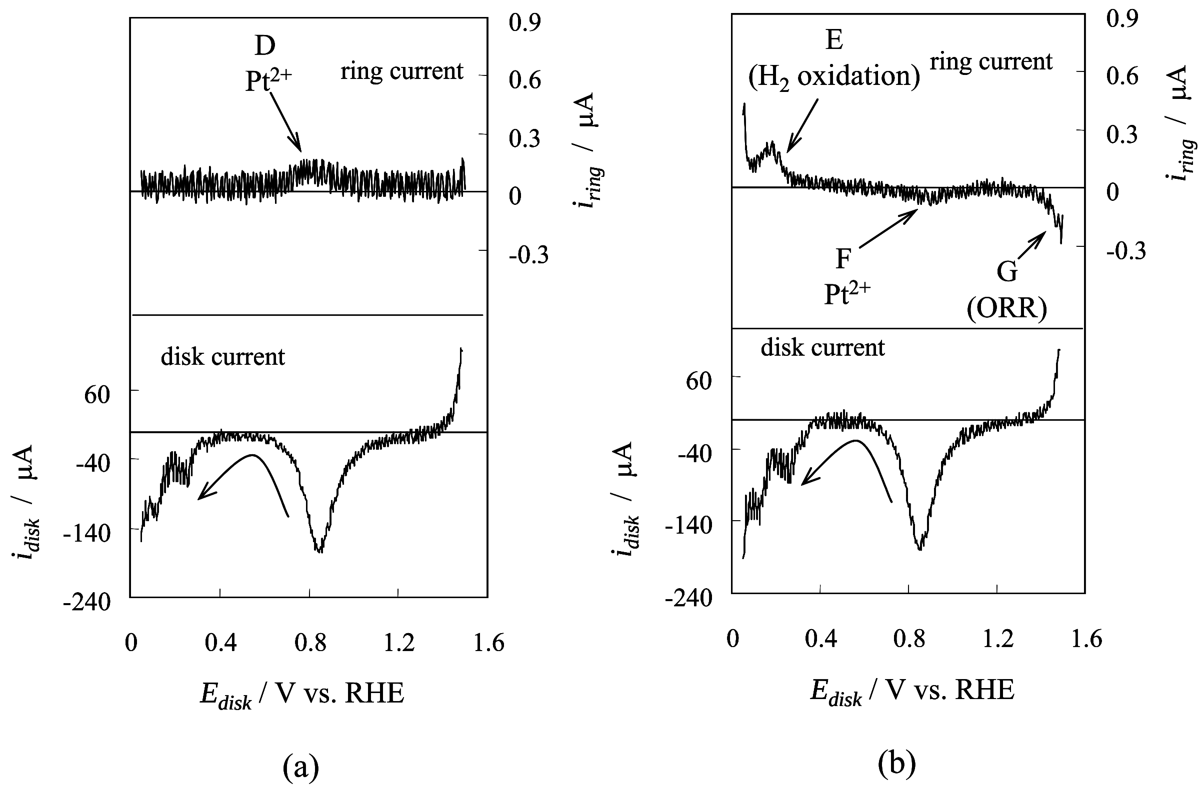

Fig.12 Cathodic sweep of the cyclic voltammograms for Pt disk and ring electrode in H_2SO_4 under nitrogen atmosphere at 40^{o}C. The potential of Pt ring electrode (a) 1.5V and (b) 0.4V.
potential range for disk electrode: 0.05-1.5V, anodic sweep rate; 10Vs^{-1}, cathodic sweep rate; 0.1Vs^{-1}

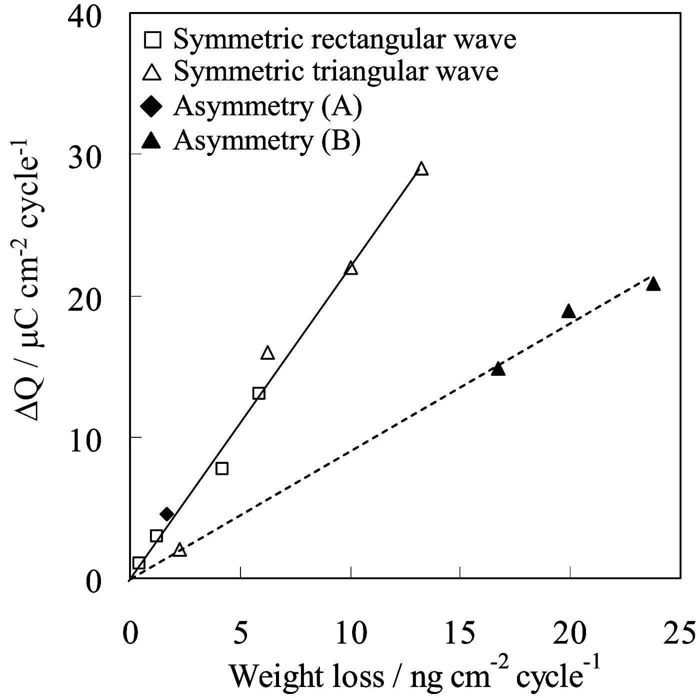

Fig. 13 Relationship between the amount of Pt consumption and the difference of the oxidation and reduction charges of Pt.